

## Rock physics modeling of a bitumen saturated reservoir with unconsolidated sands

Evan Mutual, David Cho and Kristopher Innanen

### ABSTRACT

Time-lapse (4D) seismic monitoring of thermal heavy oil production represents a simple and cost-effective method of characterizing the spatial changes in reservoir conditions due to steam injection. Using 4D AVO inversion techniques, we can estimate the changes in elastic properties due to production. To understand these elastic property changes in terms of more meaningful petrophysical parameters, we must consider the rock physics associated with our reservoir. Conventional reservoir targets can typically be modeled with standard sand and shale parameters using Batzle-Wang (1992) or Gassmann (1951) to investigate the fluid effects. In shallow heavy oil reservoirs such as the McMurray formation, the rock physics are more complex and these standard relationships are insufficient. In this study, a 4D rock physics model is created that accounts for both the unconsolidated nature of our reservoir and the finite shear modulus associated with the quasi-solid bitumen. This modeling is essential in interpreting 4D AVO inversion results and can be used as an input to a 4D rock physics inversion.

### INTRODUCTION

4D seismic monitoring of thermal heavy oil production is becoming increasingly important as companies seek to improve their operational efficiencies. This technology can offer insight into the effectiveness of the development plan by detecting residual oil saturation or areas where anomalous pressures are present. Conventional 4D seismic analysis compares amplitudes between baseline and monitor surveys to map the spatial extent of areas affected by steaming and production. Unfortunately, these amplitudes differences are not able to distinguish the physical cause of these differences. By applying more advanced technologies such as 4D AVO inversion, we can estimate the changes in elastic properties and furthermore, with the use of rock physics, we can interpret the changes in petrophysical parameters that ultimately caused the observed changes in seismic amplitudes. In this study, a new rock physics modeling workflow is introduced that accounts the unconsolidated rock physics associated with shallow, high porosity reservoirs and considers the time-lapse effects of the elastic changes due to pore fluid changes with pressure and temperature.

### METHODS AND RESULTS

The rock physics model used for this study was a non-linear regression based model that obeys physical bound theory and honors single and multi-mineral fluid substitution theory. The rock physics model is given by

$$\frac{1}{M+M_0} = \sum(1 - \varphi) \frac{v_i}{M_i+M_0} + \frac{\varphi}{M_{fluid}+M_0}, \quad (1)$$

where  $M$  is an elastic (bulk or shear) modulus,  $\varphi$  is porosity,  $v_i$  is the volumetric fraction of the  $i$ th mineral,  $M_i$  is the elastic (bulk or shear) modulus of the  $i$ th mineral,  $M_{fluid}$  is

the elastic modulus of the fluid and  $M_0$  is a regression parameter that allows local trends of the field to be captured such pressure or temperature affecting the mineral moduli. As the elastic properties of quartz are well established, we can generally use standard values of the bulk and shear moduli to describe our quartz/sand mineral end member to help constrain the model. Other more variable minerals, such as clay, which can include several different minerals, such as illite, smectite, kaolinite etc. are regressed using equation 1 to obtain an effective mineral end member.

It is well established that bitumen in Alberta's oil sands behaves as a quasi-solid at in-situ conditions due to its high viscosity. This means that the bitumen has a finite shear modulus contributing to the rock's effective shear modulus. As such, at in-situ conditions, the bitumen does not obey Batzle-Wang (1992) or Gassmann (1951) relationships and must be accounted for as a separate mineral in our rock physics modeling. To do this, we must re-normalize our petro-physical logs to yield a bitumen volume that can be considered as a third mineral end-member in addition to our sand and shale volumes. Figures 1 and 2 show tracks of various well log properties before and after the re-normalization.

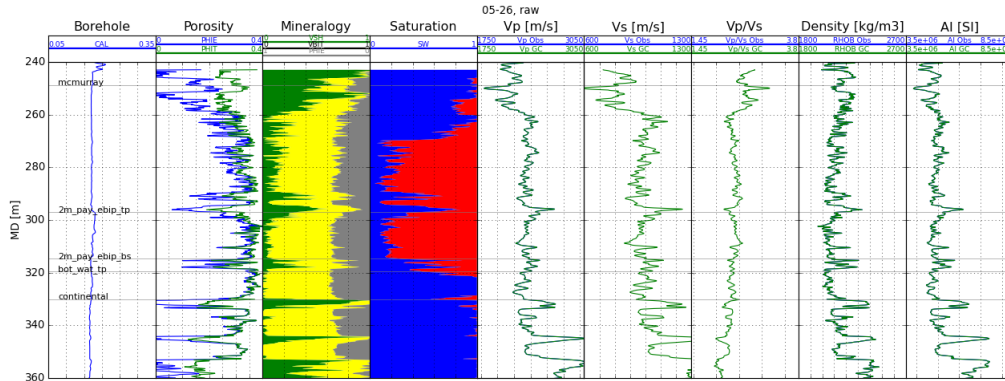


FIG 1: Well track showing petro-physics before re-normalization.

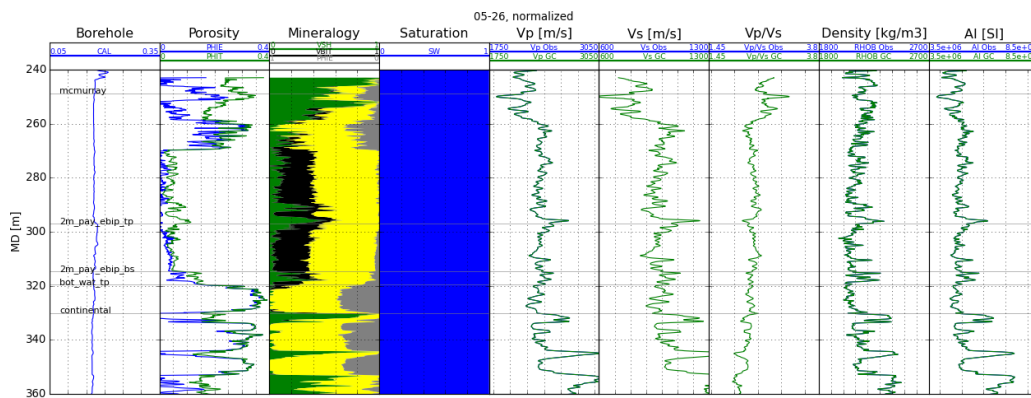


FIG 2: Well track showing petro-physics after re-normalization.

Next, the log data were QCed in various Vp cross-plot domains to identify anomalous data points and/or trends. Figure 3 shows cross-plots of Vs vs Vp for 2 wells colour

coded by various petro-physical parameters. Also plotted are theoretical Greenberg-Castagna (1992) trend lines for sand, shale and mudrock in red, green and black, respectively. As the McMurray formation is a two mineral sand/shale reservoir, we expect that the data would generally fall within the bounds of these theoretical lines. Unfortunately, even in areas with no bitumen saturation, we observe significant deviations from these trends. In particular, the data is generally observed to have a higher  $V_p/V_s$  than theory predicts. To examine the cause of this phenomenon, we must consider the assumptions made in the Greenberg-Castagna model. This model is said to hold true for consolidated rocks with moderate porosities; however, the McMurray formation is unconsolidated with porosities above thirty percent. Avseth et al. (2005), Bachrach et al. (2008) and Milovac (2009), among others, have noted that in such reservoirs, we generally observe higher  $V_p/V_s$  than predicted by standard rock physics models due to a lower shear modulus. As such, if we were to use the standard modulus of 44GPa for sand to constrain our rock physics model, we would tend to under-estimate the shear moduli of our other mineral end members in our regression. To account for this phenomenon, we will consider the workflow and derivation described by Bachrach (2008).

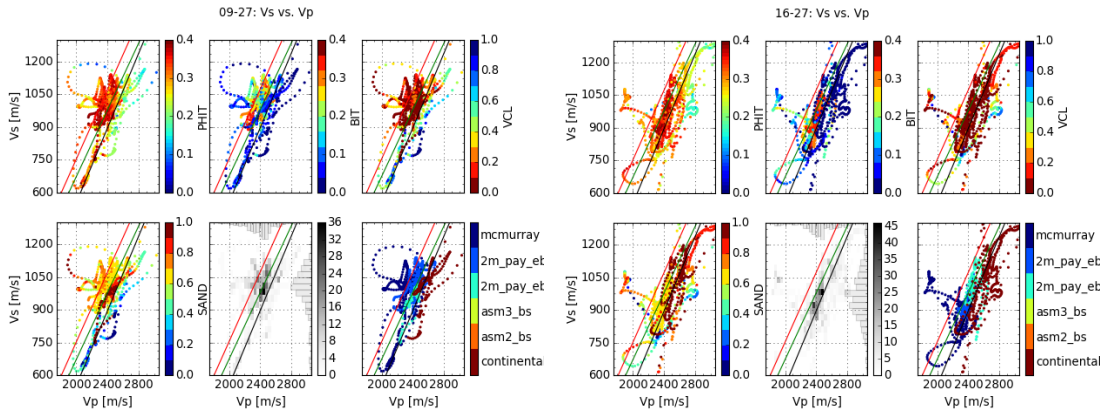


FIG 3: Vs vs. Vp cross-plots for two wells colour coded by petrophysical parameters and tops.

### Unconsolidated rock physics modeling

In the following, we provide a short review on the theory and workflow of Bachrach (2008). Consider the normal and tangential stiffness given by

$$S_n = \frac{\partial F_n}{\partial \delta}, \quad S_t = \frac{\partial F_t}{\partial \tau}, \quad (2)$$

where  $F_n$  and  $F_t$  are the normal and tangential components of the force acting on a grain contact, and  $\delta$  and  $\tau$  are the normal and tangential displacement resulting from the applied force. If we then consider our grain matrix to be adequately modeled as two elastic spheres we can describe the normal stiffness using the Hertz-Mindlin (1949) contact model defined as

$$S_n = \frac{4aG}{1-\nu}, \quad (3)$$

where  $G$  is the mineral's shear modulus,  $\nu$  is the mineral's Poisson's ratio and  $a$  is the contact radius between two spheres. We then consider the tangential stiffness defined in the Mindlin (1949) model given by

$$S_t = \frac{8aG}{2-\nu}, \quad (4)$$

Finally, we can define our effective bulk and shear mineral moduli described by Walton (1987) for a dry, dense, random pack of identical elastic spheres given by

$$K_{eff} = \frac{n(1-\varphi)}{12\pi R} S_n, \quad G_{eff} = \frac{n(1-\varphi)}{20\pi R} (S_n + 1.5f_t S_t), \quad (5), (6)$$

where  $\varphi$  is porosity,  $R$  is the grain radius,  $n$  is the coordination number and  $f_t$  is the volume fraction of non-slip contacts. We can then re-write the effective Poisson's ratio in terms of  $f_t$  yielding the following expression

$$\nu_{eff} = \frac{S_n - f_t S_t}{4S_n + f_t S_t} = \frac{2-\nu}{4(2-\nu) + 2f_t(1-\nu)} - \frac{2f_t(1-\nu)}{4(2-\nu) + 2f_t(1-\nu)}, \quad (7)$$

This equation can now be used to get an estimate for the fraction of non-slip contacts in our reservoir. The shear modulus of our unconsolidated sand mineral is then calculated using equation 7 and the following expression. Taking the lower bound where we assume zero tangential stress (or fraction of non-slip contacts equal to zero) we obtain

$$\nu_{eff} = \frac{S_n}{4S_n} = 0.25, \quad \mu_{uncon\ sand} = \frac{3K_{sand}(1-2\nu_{eff})}{2(1+\nu_{eff})} = 22.2\text{Gpa}, \quad (8)$$

Combined with our calculated value for  $f_t$  we now obtain an effective sand mineral end member estimate that is more representative of our in-situ conditions. At this point, it is important to note that these equations do not account for any fluid effects and are therefore only valid in the dry case. As such, prior to their use in any estimation using log data we must first use Gassmann theory to derive the dry Poisson's ratio.

To demonstrate the unconsolidated rock physics affecting our reservoir, synthetic shear logs were generated using theoretical Greenberg-Castagna relations and using our newly derived unconsolidated relationships. The regressed value for volume fraction of non-slip contacts was calculated to be 0.37. The results are shown in Figure 4. We can see that in general, in our sand zones, the misfit between the observed and modeled shear data has decreased. Part of the remaining misfit is due to the finite shear modulus associated with our bitumen that has not been yet been accounted for. It is also possible that the quasi-solid behaviour of the in-situ bitumen in some areas can act as cement for the grain matrix thereby making its response more similar to that of a typical, consolidated lithic rock. A fully calibrated model would ideally have a third mineral class of unconsolidated sand for each data point in our reservoir. Unfortunately, the theory for unconsolidated multi-mineral mixing in the presence of shale has not yet been well developed and is beyond the scope of this paper. The regression in this study to yield the fraction of non-slip contacts was therefore performed by removing data points with volumetric clay fractions greater than 0.2 and volumetric bitumen fractions greater than 0.3 to constrain our data to the most well behaved, predictable set of points.

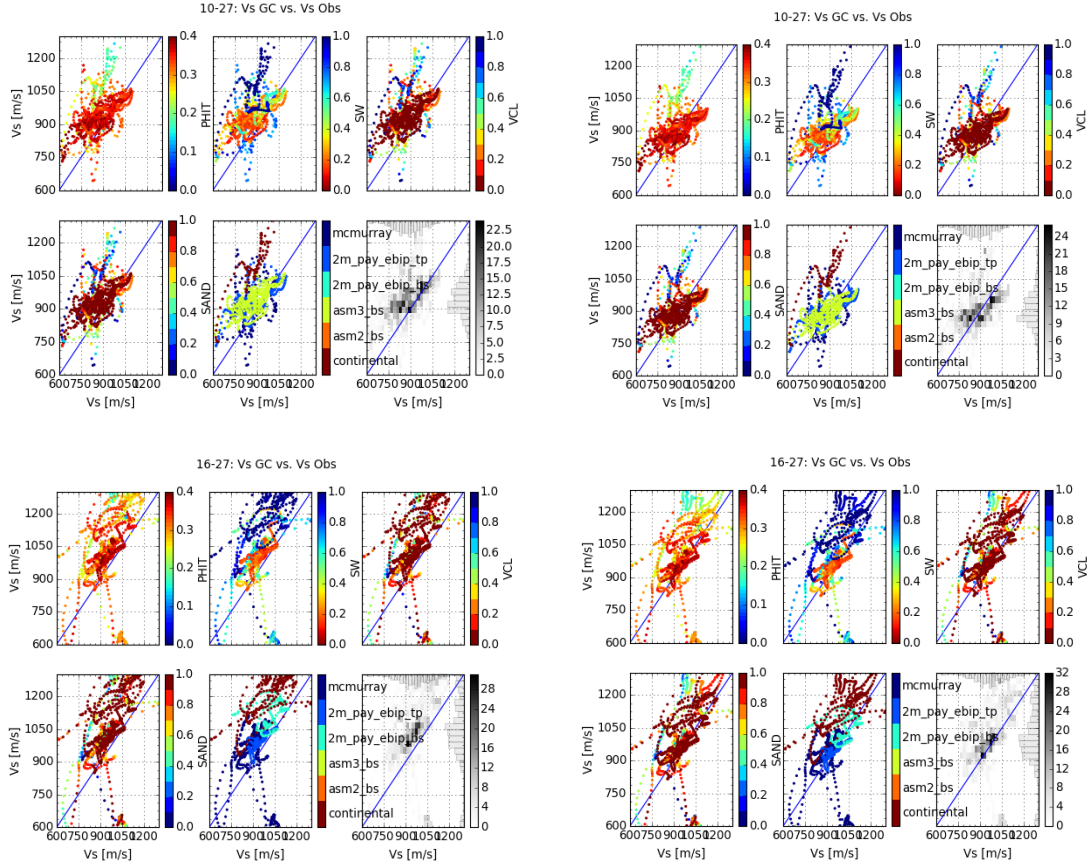


FIG 4: Modeled vs. observed shear wave velocity before (left) and after (right) inclusion of volume fraction of non-slip contacts colour coded by petro-physical parameters.

Now that we have obtained a more appropriate quartz end member for our rock physics modeling, we can derive a rock physics model using equation 1. The results for the in-situ mineral moduli are in Table 1, observed vs. modeled bulk and shear modulus are shown in Figure 5 and observed and modeled data in  $V_p/V_s$  vs. AI space are shown in Figure 6.

Table 1: Elastic moduli and densities of mineral end members

Mineral	Bulk Modulus (GPa)	Shear Modulus (GPa)	Density (g/cc)
Sand	37	44	2.650
Unconsolidated Sand	37	22.2	2.650
Shale	21.8	2.7	2.600
Bitumen	4.5	0.4	1.024

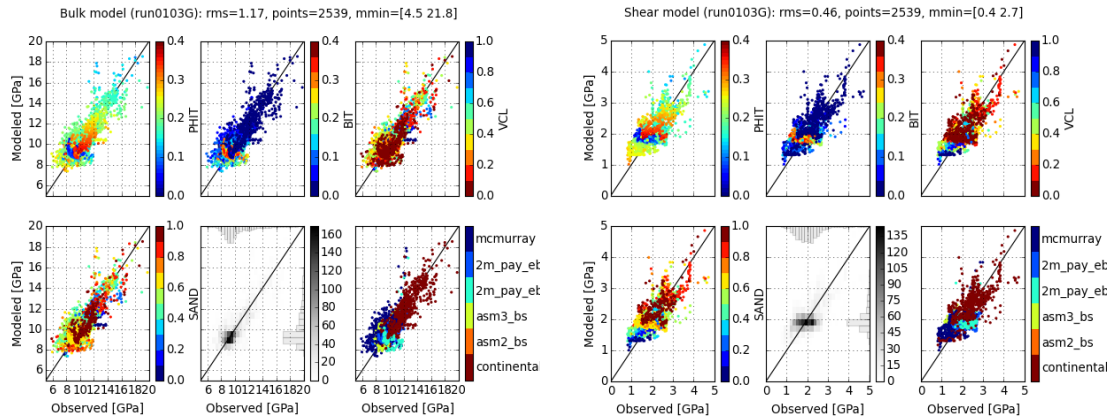


FIG 5: Modeled vs. observed bulk (left) and shear (right) modulus colour coded by petro-physical parameters.

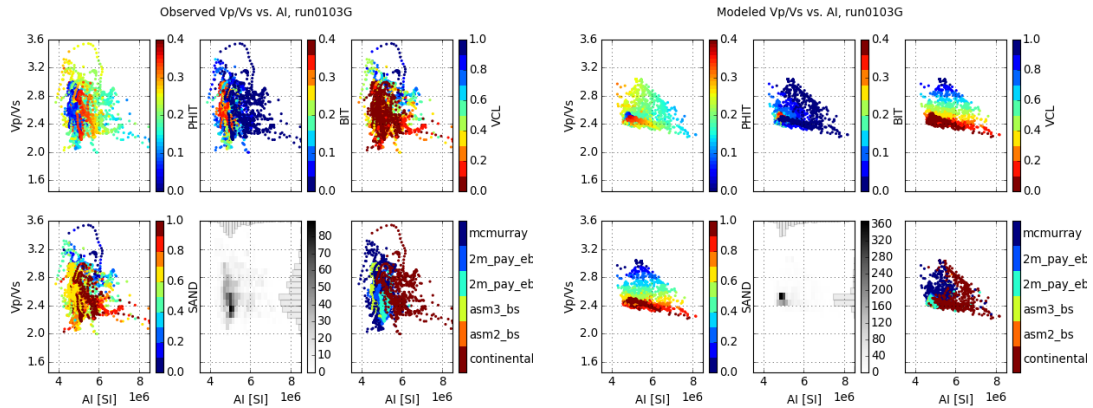


FIG 6: Observed (left) and modeled (right) data in Vp/Vs vs. AI space colour coded by petro-physical parameters.

#### 4D Rock physics modeling

Next, we consider what the rock physics response will be in a time-lapse sense. In an ideal circumstance, we would have several sets of measurements of our elastic properties for different phases of production, but in this case these calibration points were not available. In the absence of monitored logged or calibrated laboratory measurements, we will refer to the literature to help in our interpretation, and ultimately, our model building.

Much work has been done in describing the effect of increasing both heat and pressure in bitumen reservoirs. Because of the highly viscous, quasi-solid nature of bitumen reservoirs, Gassmann theory does not apply, therefore standard fluid substitution techniques are not appropriate for use in building our time-lapse rock physics model. Kato et al. (2008) illustrates the effects experimentally in a step-by-step process considering first pressure, then temperature and finally, fluid substitution. By measuring P and S wave velocities while incrementally increasing first pressure, then temperature, then water saturation, Kato was able to derive experimental relationships relating Vp and Vs for different pressure and temperature conditions. The results of the experiment are

shown in Figure 7. The most dramatic observable effect, and one that is specific to oil sands reservoirs, is during the heating process. As the bitumen is subject to heat, its shear modulus rapidly decreases to zero, thereby dramatically increasing the rock’s effective  $V_p/V_s$  ratio, while also decreasing the rock’s P-wave velocity and by extension, the acoustic impedance. This large increase in  $V_p/V_s$ , coupled with a decrease in AI, is the signature of heated, movable oil in our reservoir. In contrast, in areas surrounding the injection wells, where steam has been added to the system, a sharp decrease in our P-wave velocity coupled with minimal effect on our S-wave velocity should yield a sharp decrease in both AI and  $V_p/V_s$  ratio. Our time-lapse rock physics model will therefore consider only these two cases with the ultimate goal of being used as an input along with 4D elastic inversion results to perform a 4D rock physics inversion that quantifies changes in fluid saturation from bitumen to heated oil and detects the addition of steam to the system.

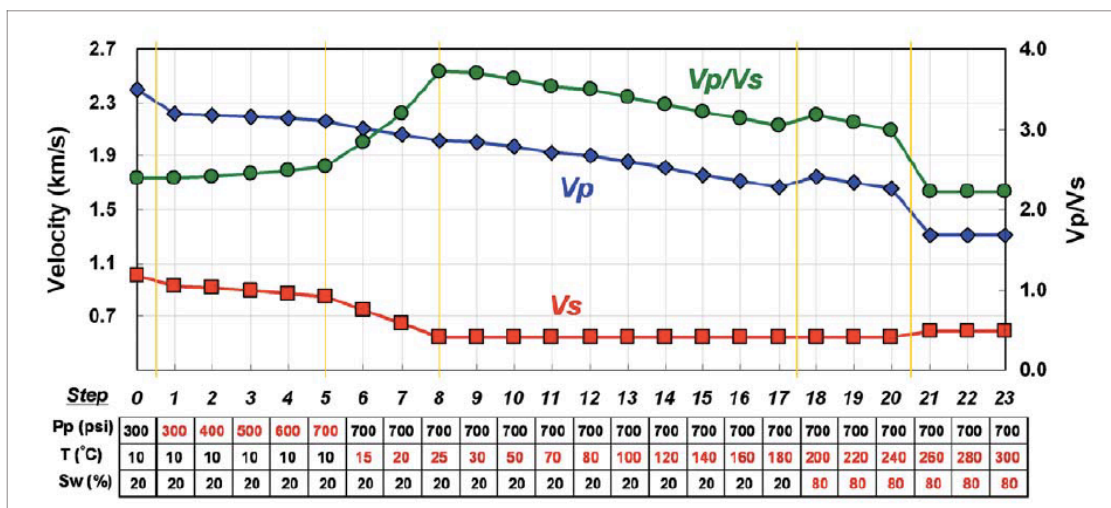


FIG 7: Sequential P and S wave and  $V_p/V_s$  ratio changes induced by steam injection. From Kato et al. (2008).

If the 4D fluid calibration data were available, it is easily incorporated into our 4D model using our in-situ sand and shale mineral end-members, which we would assume as being unchanged due to pressure and temperature conditions, and substituting all the bitumen in our well log data with heated oil, steam or gas parameters. Unfortunately, we do not have available lab data for the oil with changes in pressure and temperature. As such, for the purposes of this study we will make use of the experimental relationships derived by Kato.

Several assumptions are made in this model derivation that differ from Kato’s experiment. First, consider that Kato’s experiment is performed in a step-wise manner. This method effectively illustrates the unique impacts of pressure, temperature and fluid effects, but in a real-world SAGD setting, many of these effects would be observed simultaneously. In particular, we recognize that in Kato’s experiment the steam effect is modeled in the last step as water is replaced by steam. In a SAGD operation, steam is injected into the reservoir at steam conditions implying that steam addition occurs simultaneously with pressure increases around the borehole. De-coupling these effects is

beyond the scope of this study, but we recognize that the dominant effect likely to be observed in our 4D seismic at the wellbore will be the steam effect. For this 4D rock physics model, we will therefore model the effect of a steam phase added to the reservoir.

To approximate the 4D response of the phase change of bitumen to heated oil we will use Kato's equations given by

$$V_{p_{oil}} = (-0.0043T + 1.04)V_{p_{obs}}, \quad (9)$$

$$V_{s_{steam}} = (-0.0239T + 1.24)V_{s_{obs}}, \quad (10)$$

where  $V_{oil}$  is the velocity (acoustic or shear) of our rock in km/s,  $T$  is temperature in degrees Celsius and  $V_{obs}$  is the observed velocity (acoustic or shear) from well logs. In this case, as we are not trying to track the progression of our velocity, but obtain a value for the end member of pure heated oil, we let the shear modulus of our fluid equal zero and use equation 9 with a temperature of 25 degrees Celsius to estimate the change in acoustic velocity. The resulting 4D rock physics model is shown in Figure 8 with porosity trend lines for brine saturated sand, brine saturated shale, bitumen saturated sand, heated oil saturated sand and steam saturated sand.

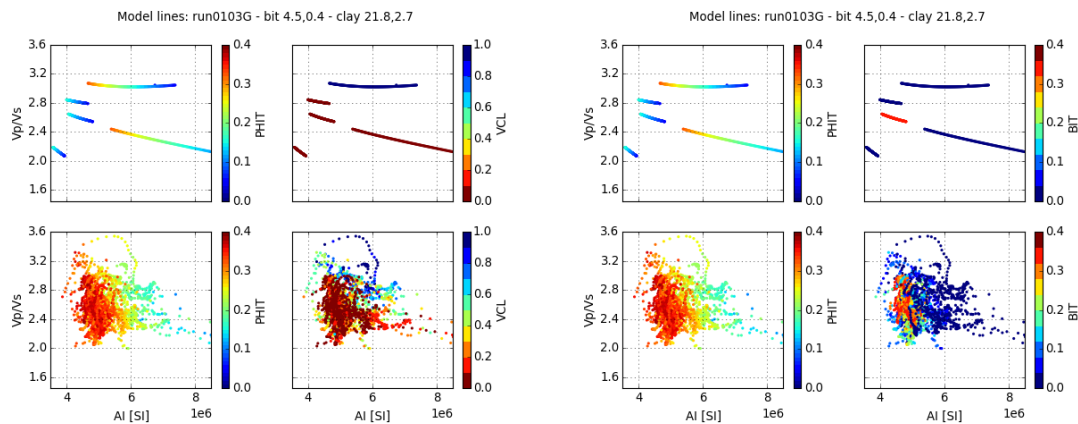


FIG 8: 4D rock physics model with porosity trend lines for brine sand, brine shale, steam sand, bitumen sand and oil sand colour coded by porosity, volume of clay and volume of bitumen.

## CONCLUSION AND FUTURE WORK

A 4D rock physics modeling workflow for thermal heavy oil was proposed that accounts for the unconsolidated mechanics of shallow reservoirs and the finite shear modulus of quasi-solid bitumen. It was demonstrated that using standard elastic moduli to describe the sand/quartz mineral end member results in over estimation of shear wave velocities. Bachrach's method was used to calculate the fraction of non-slip contacts in our reservoir to obtain a more realistic sand model thereby improving our in-situ rock physics model. Subsequently, we can use a mineral-fluid substitution of our bitumen mineral with heavy oil and steam to model an expected 4D response due to heating and steaming of a reservoir. At this point, the resulting model created in this study can be used as an interpretation aid for elastic property changes, but without proper calibration from lab measurements using such a model for a rock physics inversion after a 4D AVO inversion would be biased and difficult to validate.



## REFERENCES

- Avseth, P., Bachrach, R., 2005, Seismic properties of unconsolidated sands: Tangential stiffness,  $V_p/V_s$  ratios and diagenesis: 75<sup>th</sup> Annual International Meeting, SEG Expanded Abstracts, 1473-1476.
- Bachrach, R., and Avseth, P., 2008, Rock physics modeling of unconsolidated sands: Accounting for nonuniform contacts and heterogeneous stress fields in the effective media approximation with applications to hydrocarbon exploration: *Geophysics*, 73, no. 6, 197-209.
- Batzle, M., and Wang, Z., 1992, Seismic properties of pore fluids: *Geophysics*, 57, 1396-1408.
- Gassmann, F., 1951, Elastic wave through a packing of spheres: *Geophysics*, 16, 673-685.
- Greenberg, M. L., and Castagna, J. P., 1992, Shear-wave velocity estimation in porous rocks; theoretical formulation, preliminary verification and applications: *Geophysics Prospecting*, 40, 195-209.
- Kato, A., S. Onozuka, and T. Nakayama, 2008, Elastic property changes in a bitumen reservoir during steam injection: *The Leading Edge*, 1124-1131.
- Milovac, J., 2009, Rock physics modeling of an unconsolidated sand reservoir: Master's Thesis, University of Houston.
- Mindlin, R. D., 1949, Compliance of bodies in contact: *Journal of Applied Mechanics*, 16, 259-268.
- Walton, K., 1987, The effective moduli of a random packing of spheres: *Journal of the Mechanics and Physics of Solids*, 33, 213-226.